Pirjo Pastila
Institute of Materials Science
Tampere University of Technology
Korkeakoulunkatu 6
33720 Tampere, Finland
e-mail: pirjo.pastila@tut.fi
Tel: + 358-3-3115 2285
Fax: + 358-3-3115 2330
(Primary Contact)

Edgar Lara-Curzio
Mechanical Characterization and Analysis Group
Oak Ridge National Laboratory
1 Bethel Valley Road
Oak Ridge, TN 37831-6069, USA
e-mail: laracurzioe@ornl.gov
Tel: +1-865-574 1749
Fax: +1-865-574 6098

Antti-Pekka Nikkilä
Institute of Materials Science
Tampere University of Technology
Korkeakoulunkatu 6
33720 Tampere, Finland
e-mail: nikkila@butler.cc.tut.fi
Tel: + 358-3-3115 2321
Fax: + 358-3-3115 2330

Tapio Mäntylä
Institute of Materials Science
Tampere University of Technology
Korkeakoulunkatu 6
33720 Tampere, Finland
e-mail: tapio.mantyla@tut.fi
Tel: + 358-3-3115 2326
Fax: + 358-3-3115 2330

Microstructure and Fracture of Some SiC-based Clay Bonded Hot Gas Filter Materials After Exposure to Thermal Cycling and/or High Temperature Water Vapour

Keywords: **SiC-based hot gas filters, strength, fracture, microstructure**

Introduction

Hot gas filtration is a technology to clean fuel gas that may help increase the efficiency of advanced coal combustion or gasification power conversion processes. Cleaning of the fuel gas is required to meet environmental regulations and to prevent corrosion and erosion of turbine blades and other downstream components (Stringer and Leitch 1992, Oakey and Fantom 1997). In hot gas filtration, the hot (300-900°C), pressurized (10-25 bar) fuel gas from the combustion process is led without cooling and reheating through the filters. Hot gas filters need to operate reliably for more than 10, 000 hours, maintaining high particulate removal efficiencies, high flow capacity and low pressure drop. They should also possess durability and reliability against mechanical and thermal stresses (Alvin et. al 1991).

Aggressive process environments containing steam, dust, gaseous sulphur and alkali cause microstructural changes in all common hot gas filter materials, including oxide, non-oxide and mixed oxide ceramics (Alvin et. Al. 1991, Oakey and Fantom 1997, Alvin 1997). These changes - crystallization, oxidation and softening of glassy phases - affect filtration efficiency, long term reliability, strength and creep properties of the filters (Alvin 1997, Spain and Starrett 1999, Alvin 1999, Pastila et. al. 1998, Oakey et. al. 1997). Uncertainties about their long-term reliable operation and unexpected failures have been restricting issues for the use of SiC-based hot gas cleaning filters especially in High-Temperature High-Pressure (HTHP) combustion processes. Degradation of the filter material due to microstructural changes during operation has been well known, but the mechanisms responsible for these changes have not been studied in detail.

Objective
The purpose of this study is to charcterize microstructural changes and analyse their possible effect to long term durability and reliability of SiC-based clay bonded hot gas filters.

Approach
The analysis of degradation mechanisms is a difficult task because the filtration environment in HTHP system is very complex, it can vary significantly with the fuel used, and it is a high-temperature high-pressure process. In this study only two of the parameters associated with the real process have been selected: the effect of water vapour and temperature changes on microstructural evolution of the filter material. These are selected since they can, even by themselves, have significant effects on SiC-based clay bonded hot gas filter material. Temperature changes through the cristobalite transformation temperature 226°C occur in service at start up-shut down transients. Water vapour is usually present both in combustion and gasification. Water vapor enhances oxidation of SiC (Jorgensen et. al. 1961, Opila 1999, Maeda et.al. 1988) and devitrification of SiO_2 scale (Jacobson 1993, Fergus and Worrell 1990, Lawson et. al. 1990).

Project Description
Two types of SiC-based clay bonded commercial grade filter materials were exposed in laboratory scale for temperature cycling at 150°C to 400°C in air, for water vapour in air at 850°C and for combined hold in water vapour at 850°C and cycling to 150°C. The coding of samples and exposure conditions are presented in more detail in Table 1. The as received material is used as reference and some of the results are compared to filters that have experienced service operation. The purpose of the exposures was to cause possible damage to the filter materials due to cristobalite $\alpha-\beta$ transformation, oxidation or crystallization of the binder phase.
To detect the possible changes due to exposures the microstructure of the filter materials has been characterized in several ways. Chemical composition was determined* by X-ray fluorescence (XRF), flame atomic adsorption spectroscopy and solid-state infrared adsorption methods. The phase composition was detected by quantitative X-ray diffraction method. Calcium fluoride (CaF_2) was mixed with the sample as an internal standard phase that against calibration curves from unknown mixture allows the calculation of the amounts of phases interested. The amounts of SiC, cristobalite and mullite were determined from the fraction of filter sample crushed and passed through the 100 μm sieve. Estimates of the filter phase compositions were generated from the sieved fraction combining the weight of removed fraction after HF etching as SiC and the weight of etched away fraction as calculated from XRD-data. SEM-study with EDS-analysis for phase detection and dilatometer study for thermal behavior will further support the microstructural analysis.
Both hoop strength and tensile strength data at room temperature were obtained as well as tensile stress-strain behavior. For hoop strength testing 20 mm wide rings were used. The exposed strength specimens were cut before exposures. The number of ring specimens tested was 30 after completed exposure and 10 or 15 at early stage of the exposure. For tensile testing 17.8 cm long tubes were cut and their ends were ground to fit the grips. Three samples were tested using clip on extensometer to record the stress strain behavior. The monotonic loading rate was 0.2 mm/s.

---

* Rautaruukki Research Center for Rautaruukki Steel, Raahe, Finland

Selected fracture surfaces were studied with SEM. The fracture toughness of the filter material was determined by means of the Chevron notch test method.

Results

Microstructure

Typical microstructures of studied materials are shown in Figure 1. According the EDS analyses from carbon coated polished cross sections the composition of the Na_2O-K_2O-Al_2O_3-SiO_2 amorphous phase is nearly identical in the materials. The grain size of mullite is larger in material A. Cristobalite is found next to SiC grains in both materials and this layer is cracked due to thermal expansion mismatch, Figure 2.

The XRD results shown in Table 2 suggest that the amount of mullite is larger in material A and the amount of cristobalite larger in material B. The absolute amounts of phases calculated from XRD results may not be exact due to restrictions of the method and sample preparation but when compared to the calculations from chemical analyses it was found that the trends of mullite and cristobalite are correct. That is, when chemical analysis suggested more mullite or crsitobalite it was so also according the XRD data. Also, the samples could be distinguished from each other correctly comparing the relative amounts of mullite and cristobalite. Since chemical analysis of the reference materials and thermally cycled materials were not satisfactory due to problems in dissolving SiC into the sample and the XRD results were capable to give nearly the same information, chemical analysis was not further used. The method at Rautaruukki Research Center is optimised for steels and only 85-93% of the filter sample was successfully analysed. The calculated phase composition from chemical analysis is also presented in Table 2.

The phase composition of exposed materials showed some changes in the amount of cristobalite and mullite, Table 2. The suggested increase in the amount of mullite after thermal cycling is not possible since the temperature was only 400ºC and questionable at 850ºC. On kinetic studies of mullite formation from aluminosilicate gels (Li 1990) showed that nucleation of mullite from the single phase gel could occur at 940ºC but sintering temperatures above 1250ºC were needed to reach completion of mullite conversion. It was also stated that the grain growth is hindered by the particle boundary of the gel and the activation energy for the inter-granular growth is higher than for nucleation. The single phase gel is an amorphous molecular level mixture of Al_2O_3 and SiO_2. Molecular mixture does occur in kaolinite clay but mixing is three dimensional in the synthesized gels and one dimensional in kaolinite (Li 1990). Thus at this moment the changes in the amount of mullite after thermal cycling are considered to be variations from sample to sample. The increase in cristobalite content after water vapor exposures is considered to be possible. Water vapor is well known to promote cyrstallization of SiO_2 at high temperatures. From outer surfaces of binder necks small crystals were found that EDS analysis revealed to be pure SiO_2, Figure 3. More crystallization occurred in filter B as suggested by XRD, it was easily observed from polished and etched cross sections, Figure 4. Note also the small crystals on the initial cristobalite layer next to SiC suggesting crystallization from the amorphous binder phase.

Strength

The studied filters were all from the same production lot to minimize possible variations in microstructure and strength. For as received filters the strength (at failure probability of 66.7%) and its 90-% confidential range, Weibull modulus and number of specimens are presented in Table 3. Strength specimens were from 6 filters of each type. From type A two kind of filters with significant difference in their strength were found. Also from type B one filter with clearly higher strength compared to others was found. Their 90-% confidential range does not overlap with others. The two original reference sets Ref 1 and Ref 2 showed

no significant variation and only the reference materials that were studied at Argonne National Laboratory with Acousto-Ultrasound revealed the problem. Additional reference sets noted Ref w and Ref w+c are from the filters where most of the strength specimens were cut for the exposures at water vapor and at vapor with cycling respectively. However, for both exposures rings were cut from three filter tubes in order to optimize the material consumption and to get representative sample of the filters.

The strength of exposed materials compared to as received strength with its 90-% confidential range is presented in Figure 5. Where available, the reference strength from the same filter tube from which the majority of the exposed strength specimens were cut is presented. The strength was found to decrease in all exposures, most significant effects were found after water vapor exposure with thermal cycling for both filter types. In all cases strength change was low, only 20% at worst. Material A maintained its better strength compared to material B even after the higher decrease in strength in the exposures. Material B had higher Weibull modulus and thus more narrow 90-% confidential range before and after exposures than material A.

Originally the thermal cycling was assumed to be responsible for an increase of the strength of material A since the strength after cycling was 25 MPa and the reference had 21 MPa (Pastila et. al 2002). Increase in strength of the same filter type has been reported after nearly 500h operation at the Karhula pilot plant (Commission of the European Communities 2002). The cycling experiment was repeated so that 40 specimens were cut from single filter and every other was exposed when the others were used as reference. The thermal cycling did decrease the strength of both filter types but by less than 10%.

Two tensile test specimens were evaluated under monotonic loading rate. The average tensile strength did follow the results of hoop strength. Tensile strength is significantly lower than hoop strength. Especially the water vapor exposed specimens had very low tensile strength. Lower strength is expected since according the Weibull theory (Weibull 1939) larger volumes of the same material should have lower strength. Compression gripping of the specimen causes multiaxial stress state and the failure occurred typically at or near the end of grip. Gripping is considered to have some contribution to lower the strength. Failures away the grips did also occur. A water vapor exposed specimen of filter B did fail away from the grip and final separation of the fracture surfaces occurred only after the test was stopped.

Figure 6 gives a summary of mechanical properties of the filters studied. The deviation in tensile strength is calculated as the difference between the average tensile strength and maximum tensile strength. Young's modulus was determined using a clip-on extensometer, the average value is given in Figure 6.

Fracture

Fracture toughness was determined by four point bending from Chevron notched specimens for filter type A. The value of fracture toughness was 0.7±0.11 for reference state material and 0.8±0.13 for thermally aged material. The number of specimens tested was 8. The reference and thermally aged specimens were not form same filter tube. Strong grain interlocking was observed, the fractured surfaces were strongly attached to each other after the test. The fracture path was found to be very tortuous.

From tensile tested specimens it was possible to calculate the Work of Fracture (WOF) which is defined as the total energy needed to produce a unit area of fracture surface (Sakai and Ichikawa 1992). The values presented in Figure 6 were calculated from the area under load displacement curve and from cross sectional area of the specimen. Note the drastic decrease in WOF for water vapor exposed specimens. When fracture surfaces of hoop strength specimens were studied with SEM it was noted that fracture between cristobalite and SiC grain was favoured in water vapor exposed specimens, especially in material A. When the

number of SiC-grains from which the binder was broken away was counted from several micrographs it was clearly higher for the vapor exposed specimens than for the reference specimens.

Application and Future Activities

The current results suggest that water vapor is capable to cause crystallization of silica from the binder phase. Decrease in strength due to exposure to thermal cycling and high temperature water vapor was found. However, the strength decrease is only 10-20% whereas SiC based clay bonded filter materials showed decrease of 30-40% after thermochemical loading at dry oxidizing environment with or without alkali loads (Westerheide at al. 2002). No microstructural changes were detected. In another study clay bonded filters from Schumacher operated up to 1500 hours at Karhula pilot plant did not show significant strength reduction. Some crystallization of silica at outer surfaces of binder phase was detected (Commission of the European Communities 2002). The current results suggest that water vapor or thermal cycling through cristobalite phase transition temperature do not lower the room temperature strength of SiC based clay bonded material significantly.

In the future the tensile behavior and slow crack growth of filter materials in high temperature water vapor environment will be studied. The combined effect of alkalis and water vapor to the microstructure and strength is then the key for life time prediction of the SiC based clay bonded hot gas filters.

References

1. Stringer, J. & Leitch, A. J., Ceramic candle filter performance at the Grimethorpe (UK) pressurized fluidized bed combustor. *J. Eng. Gas Turbine Power-T ASME*, 1992, **114**, 371-378.
2. Oakey, J. E., Fantom & I. R., Hot gas cleaning - materials and performance. *Materials at high temperatures*, 1997, **14**, 337-345.
3. Alvin, M. A., Lippert T. E. & Lane, J. E., Assessment of porous ceramic materials for hot gas filtration applications. *Am. Ceram. Soc. Bull.*, 1991, **70**, 1491-1498.
4. Alvin, M. A., Performance and stability of porous ceramic candle filters during PFBC operation. *Materials at high temperatures*, 1997, **14**, 355-364.
5. Spain, J. D. & Starrett, H. S., Characterization of monolithic and composite filter elements. In *High temperature Gas Cleaning Volume II*, ed. A. Dittler, G. Hemmer and G. Kasper. Institut für Mechanische Verfarenstechnik und Mechanik der Universität Karlsruhe (TH), Karlsruhe, 1999, pp. 414-427.
6. Alvin, M. A., Hot gas filter development and performance. In *High temperature Gas Cleaning Volume II*, ed. A. Dittler, G. Hemmer and G. Kasper. Institut für Mechanische Verfarenstechnik und Mechanik der Universität Karlsruhe (TH), Karlsruhe, 1999, pp. 455-467.
7. Pastila. P. H., Nikkilä, A.-P., Mäntylä T. A., The effect of oxidation on creep of clay bound SiC filters. *Ceram. Eng. Sc. Proc.*, 1998, **19**, 37-44.
8. Oakey, J. E., Lowe, T., Morrell, R., Byrne, W. P., Brown, R. & Stringer, J., Grimethorpe filter element performance – the final analysis. *Materials at high temperatures*, 1997, **14**, 371-381.
9. Jorgensen, P. J., Wadsworth, M. E. & Cutler, I. B., Effects of water vapour on oxidation of silicon carbide. *J. Am. Ceram. Soc*., 1961, **44**, 258-261.
10. Opila, E. J., Variation of oxidation rate of silicon carbide with water-vapour pressure. *J. Am. Ceram. Soc*., 1999, **82**, 625-636.

11. Maeda, M., Nakamura, K. & Ohkubo, T., Oxidation of silicon carbide in a wet atmosphere. *J. Mat. Sci*., 1988, **23**, 3933-3938.
12. Jacobson, N. S., Corrosion of silicon-based ceramics in combustion environments. *J. Am. Ceram. Soc*., 1993, **76**, 3-28.
13. Fergus, J. W. & Worrell, W. L., The oxidation of chemically vapour deposited silicon carbide. In *Ceramic Transactions vol. 10 Corrosion and corrosive degradation of ceramics*, Ed. R. E. Tressler and M. McNallan. American Ceramic Society, Westerville, OH, 1990, pp.43-51.
14. Lawson, M. G., Kim, H. R., Pettit, F. S., & Blachere, J. R., Hot corrosion of silica. *J. Am. Ceram. Soc*., 1990, **73**, 989-995.
15. Li, D. X., Kinetic studies of mullite formation from aluminosilicate gels, Ph D dissertation, Washington State University, Department of Chemical Engineering, August 1990.
16. Pastila P., Lara-Curzio E., Nikkilä A.-P. & Mäntylä T., Effect of thermal cycling to the stregth and fracture of SiC-based candle filters, to be published in *Ceram. Eng. Sc. Proc.* 2002.
17. Commission of the European Communities Directorate-General for Energy, Demonstration of hot-gas cleaning with hanging and upright ceramic filter candles, Final technical report, Phase II, Berlin 2002.
18. W. Weibull, A Statistical Theory of the Strength of Materials, Ingenörsvetenskapsakademiens handlingar nr 151, 1939.
19. M. Sakai and H. Ichikawa, Work-of-fracture of brittle materials with microcracking and crack bridging, *International Journal of Fracture*, 1992, **55**, 65-79.
20. Westerheide, R., Rehak, P., Adler, J., Angerman, J., & Meyer, B., Effect of combustion conditions on properties of ceramic hot gas filters, to be published in *Ceram. Eng. Sc. Proc.* 2002.

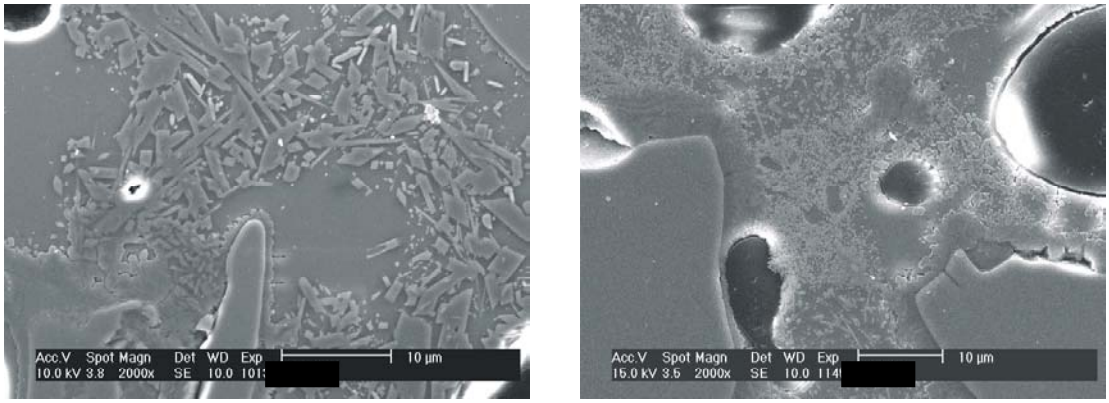

A B

Figure 1. Typical HF-etched cross sections of binder in filters studied. On the left material A, on the right material B.

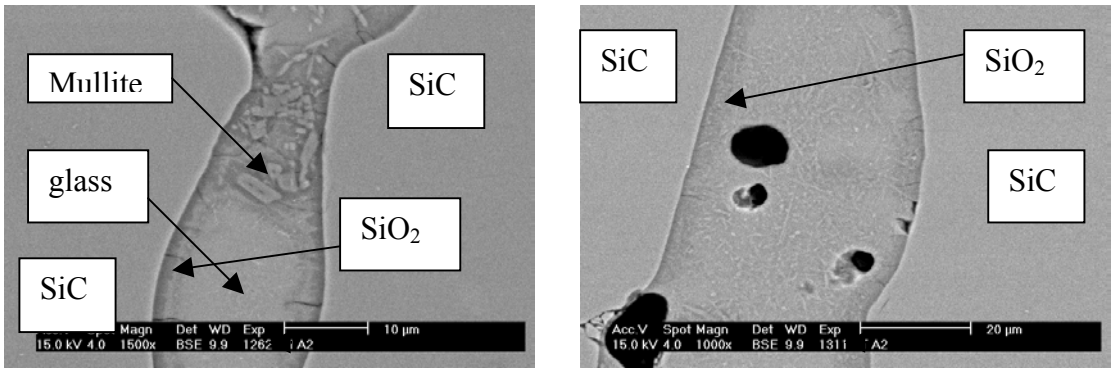

A B

Figure 2. Backscattering images of polished cross sections. On the left material A on the right material B. Pure SiO_2 is found next to SiC grains, the dark phase with cracks.

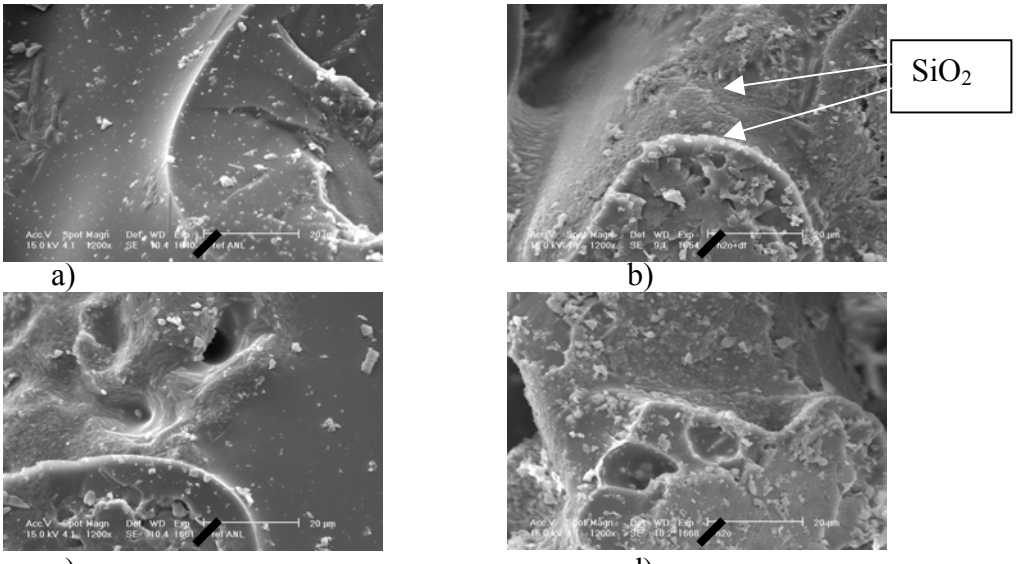

a) b)

c) d)

Figure 3. SEM images of binder outer surface. a) Material A reference, b) material A water vapor and cycling, c) material B reference, d) material B water vapor.

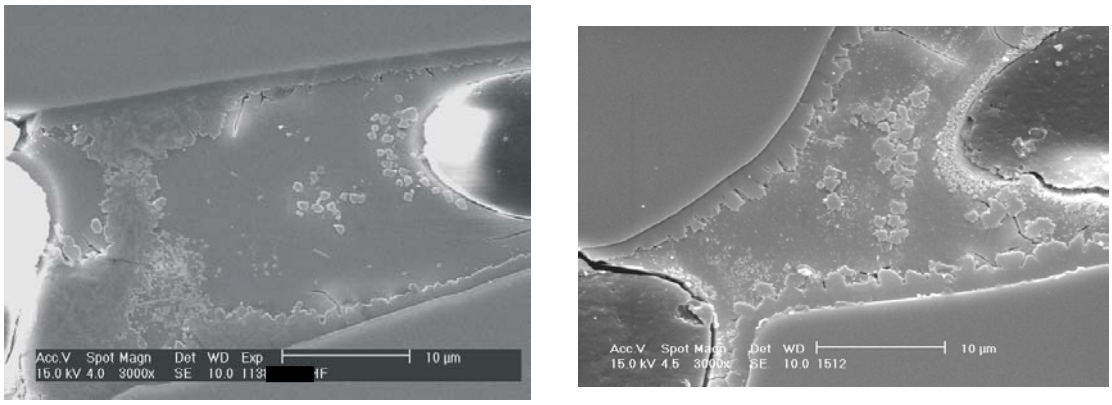

Figure 4. SEM images from polished and HF etched cross sections of filter B. On the left reference material, on the right after 500h hold at 850ºC water vapor.

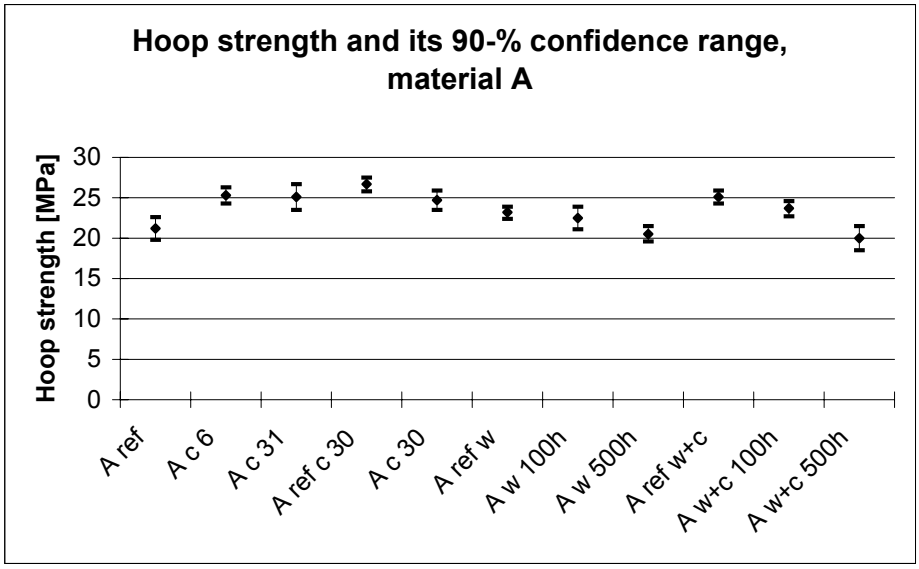

Figure 5a. Hoop strength and its 90-% confidence range of material A. Exposures are thermal cycling c with number of cycles, hold at water vapor w with time, and hold at water vapor w+c with 4 and 8 thermal cycles.

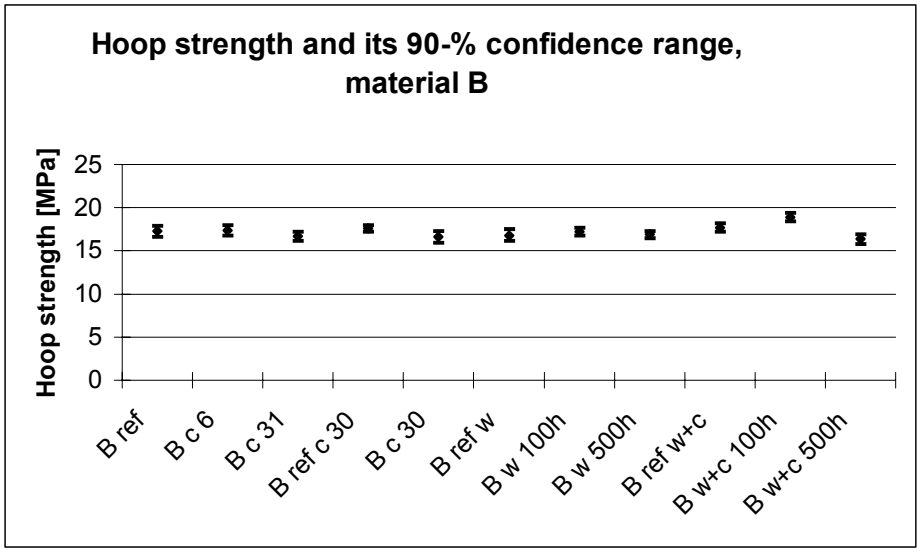

Figure 5b. Hoop strength and its 90-% confidence range of material B. Exposures are thermal cycling c with number of cycles, hold at water vapor w with time, and hold at water vapor w+c with 4 and 8 thermal cycles.

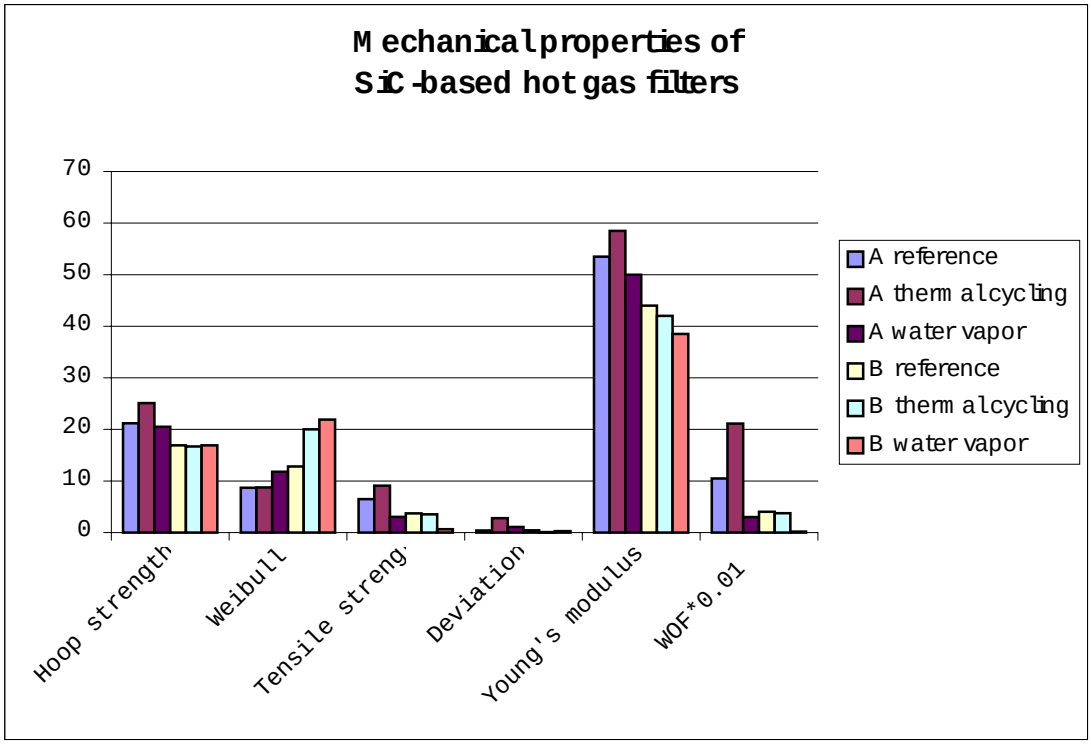

Figure 6. Summary of the mechanical properties of the filters studied

Table 1. Exposure environments. Specimens removed at early state / specimens completed the exposure.

Exposure	Time at max. T	Temperature ºC	No of cycles	Water feed into chamber
Thermal cycling (c)	**24/124h**	**150-400**	**6/31**	**No**
Water vapor (w)	**100/500h**	**850**	**-**	**Yes (2 ml/min)**
Water vapor and cycling (w+c)	**95/455h**	**100-850**	**4/8**	**Yes (2 ml/min)**

Table 2. Phase composition of materials A and B with standard deviations. Composition is calculated from XRD data of sieved fraction combined with weight data of coarse fraction after HF etching. Calculation of the phase composition from chemical analysis is based on the composition of the amorphous binder according to EDS and the amount of SiC according the carbon content of the samples given in chemical analysis.

Sample	**Composition in wt.-% ± standard deviation**			
	SiC	Mullite	Cristobalite α+β	Amorphous
A reference	82.9±0.92	1.6±0.55	0.6±0.10	14.9±0.88
Chemical analysis	*77.8*	*5.8*	*1.0*	*15.4*
A thermal cycling	85.5±2.78	3.3±0.53	1.1±0.14	10.1±3.41
Chemical analysis	*78.4*	*6.2*	*0.8*	*14.6*
B reference	84.7±0.69	1.3±0.48	1.4±0.10	12.6±0.92
Chemical analysis	*82.8*	*4.2*	*4.6*	*8.4*
B thermal cycling	85.7±5.66	2.2±0.26	2.3±0.10	9.8±5.41
Chemical analysis	*83.7*	*4.2*	*3.7*	*8.4*
A water vapor	78.8±1.61	2.6±0.08	0.9±0.12	17.6±1.37
A vapor+cycling	51.3±8.42	3.5±0.52	1.6±0.10	43.8±8.50
B water vapor	85.3±1.13	2.0±0.47	2.6±0.36	10.1±1.26
B vapor+cycling	73.0±1.01	1.9±0.17	3.1±0.09	22. 0±1.08

Table 3. Modulus of Rupture strength, its 90% confidence range, Weibull-modulus and the number of specimens tested for reference state filter materials taken from several as received filter tubes.

Sample	Strength [MPa]	90% conf. range [MPa]	Weibull modulus	No. of specimens
A REF 1	21.2	19.8-22.6	7	30
A REF ANL	25.2	24.1-26.2	13	19
A REF W+C	25.1	24.3-25.9	17	14
A REF W	23.2	22.4-23.9	18	12
A REF 2	22.6	21.8-23.5	15	12
A REF 3	26.7	25.8-27.5	17	20
B REF 1	17.3	16.6-17.9	14	30
B REF ANL	19.4	19.1-19.7	37	12
B REF W+C	17.7	17.2-18.2	21	14
B REF W	16.8	16.2-17.5	15	13
B REF 2	17.7	17.2-18.3	18	9
B REF 3	17.6	17.2-18.0	25	20